Journal of Organometallic Chemistry, 430 (1992) 221–234
Elsevier Sequoia S.A., Lausanne
JOM 22488

Heteronuclear clusters containing the hexafluorobut-2-yne ligand. Crystal structures of $(C_5H_5)_2Rh_2Pt(CO)(CF_3C_2CF_3)(COD)$ (2) and $(C_5H_5)_4Rh_4Pt(CO)_2(CF_3C_2CF_3)_2$ (3), and facile Rh–Pt bond making and breaking for complex 2 in solution

Ron S. Dickson, Gary D. Fallon, Kerryn D. Heazle and Michael J. Liddell
Department of Chemistry, Monash University, Clayton, Victoria 3168 (Australia)

(Received October 14, 1991)

Abstract

The hetero-trinuclear cluster $(C_5H_5)_2Rh_2Pt(CO)(CF_3C_2CF_3)(COD)$ (**2**) is formed when equimolar amounts of $(\eta\text{-}C_5H_5)_2Rh_2(\mu\text{-}CO)(\mu\text{-}\eta^2\text{-}CF_3C_2CF_3)$ and $Pt(COD)_2$ are mixed in solution at room temperature. The structure of **2** has been determined by X-ray crystallography and reveals an open V-shaped arrangement of the metal atoms with one Rh–Rh and only one Rh–Pt bond. There is a semi-triply bridging attachment of the carbonyl, with a very long Pt–CO distance (2.658(8) Å). The alkyne is σ-bonded to Pt and one Rh and π-attached to the remaining Rh. Spectroscopic data support the co-existence of two isomers in solution. In one, the solid state structure is retained; the other has a closed Rh_2Pt core and the alkyne rotates freely on this face at room temperature. If the initial reaction is done with a deficiency of $Pt(COD)_2$, or when $Pt(NBE)_3$ is treated with $(\eta\text{-}C_5H_5)_2Rh_2(\mu\text{-}CO)(\mu\text{-}\eta^2\text{-}CF_3C_2CF_3)$, a hetero-pentanuclear cluster $(C_5H_5)_4Rh_4Pt(CO)_2(CF_3C_2CF_3)_2$ (**3**) is formed. The crystal structure of **3** has also been determined and shows that it has a metal core consisting of two Rh_2Pt triangles sharing a common Pt. The carbonyl is asymmetrically bonded to the longest Rh–Pt edge within each triangle, and the alkyne is attached in the $\mu_3\text{-}(\eta^2\text{-}//)$ mode. This structure is retained in solution.

Introduction

The design of heteronuclear clusters can be approached in a number of ways [1]. One that has been developed extensively involves the use of metal complexes as ligands that can be added to other complexes [2]. In the present paper, we establish that this approach can be extended to the preparation of clusters in which an alkyne is attached to a heteronuclear M_2M'-face. Our syntheses are based on the stepwise displacement of the labile 1,5-cyclooctadiene (COD) ligand(s)

Correspondence to: Dr. R.S. Dickson, Department of Chemistry, Monash University, Clayton, Victoria 3168, Australia.

from $Pt(COD)_2$ by additions of the dinuclear alkyne complex $(\eta\text{-}C_5H_5)_2Rh_2(\mu\text{-}CO)(\mu\text{-}\eta^2\text{-}CF_3C_2CF_3)$; clusters with alkyne-$Rh_2Pt$ faces are obtained. There is considerable current interest in alkyne-cluster complexes, particularly those with two or more different metals, and recently [3] we drew attention to the reasons for this.

Experimental section

General procedures

The manipulation of all compounds was carried out under prepurified nitrogen in standard Schlenk-type glassware. Preparative-scale thin-layer chromatography was performed on 20×20 cm plates with a 1:1 silica gel G-HF_{254} mixture as adsorbent. All separations were achieved on plates that had been dried in the air at room temperature. The reported microanalyses were performed by the National Analytical Laboratories Pty. Ltd., Victoria, Australia.

Reagent grade solvents were purified by standard procedures [4] and were stored in the dark over activated 4A molecular sieves (CH_2Cl_2) or Na wire (hexane, pentane); they were degassed and saturated with nitrogen before use. $RhCl_3 \cdot xH_2O$ was obtained from Johnson Matthey and was used to prepare $(\eta\text{-}C_5H_5)_2Rh_2(CO)(CF_3C_2CF_3)$ according to the published method [5]. Standard literature procedures were used to prepare $Pt(COD)_2$ [6] and $Pt(NBE)_3$ [7].

Instrumentation

Infrared absorption spectra were recorded on a Perkin–Elmer 1600 FTIR spectrometer. NMR spectra were measured on a Bruker AM-300 spectrometer. The ^1H NMR spectra were measured at 300 MHz, ^{19}F at 282.4 MHz, and ^{13}C at 75.5 MHz; deuterated solvents ($CDCl_3$, acetone-d_6) were used as internal locks. Chemical shifts are in parts per million from internal Me_4Si for ^1H and ^{13}C and from CCl_3F for ^{19}F; in all cases, a positive chemical shift denotes a resonance downfield from the reference. In obtaining ^{13}C NMR spectra, $Cr(acac)_3$ was added to reduce T_1 relaxation times. Mass spectra were recorded on a VG Micromass 7070-F spectrometer. The FAB mass spectra were kindly provided by Dr. C. Adams, University of Adelaide; the spectra were obtained on a VG ZAB 2HF instrument equipped with a FAB source.

Reaction of $(\eta\text{-}C_5H_5)_2Rh_2(CO)(CF_3C_2CF_3)$ (1) with $Pt(COD)_2$, 1:1 ratio

A solution of **1** (0.050 g) in hexane (20 ml) was added slowly to a stirred solution of $Pt(COD)_2$ (0.043 g; mol ratio 1.0:1.1) in hexane (20 ml). The reaction flask was kept in the dark. Some large green-black crystals were deposited within 24 h, and crystallization was complete in about 7 days. The crystals were isolated by decantation and were washed with pentane and dried under vacuum. This gave $(\eta\text{-}C_5H_5)_2Rh_2Pt(CO)(CF_3C_2CF_3)(COD)$ (0.035 g, 42%), m.p. 170°C. Anal. Found: C, 33.7; H, 2.6; F, 14.2. $C_{23}H_{22}F_6OPtRh_2$ calc.: C, 33.3; H, 2.7; F, 13.8%. Mass spectrum, *m/z* (relative intensity, assignment): 829 (4%, *M*), 694 (10%, $[(C_5H_5)_3Rh_3(CO)(CF_3C_2CF_3)]^+$), 666 (12%, $[(C_5H_5)_3Rh_3(CF_3C_2CF_3)]^+$), 233 (100%, $C_{10}H_{10}Rh^+$). Infrared spectrum: ν(CO) at 1789vs (KBr) or 1761s (CH_2Cl_2

soln.) cm^{-1}. ^1H NMR spectrum ($CDCl_3$): δ 5.38 (m, 14H, $(C_5H_5)_2 + (=CH)_4$ of COD), 2.15 (m br, 8H, $(CH_2)_4$ of COD. ^1H NMR spectrum (acetone-d_6): (C_5H_5) resonances of relative intensity 5:5:10 at δ 5.60 (s), 5.44 (d, J(Rh–H) = 0.8 Hz), 5.37 (s), and COD resonances at δ 7.69 (m, 1H), 6.23 (td, 1H), 5.04 (m, 1H), 4.65 (m, 2H), 4.49 (qd, 1H), 4.22 (dd, 1H); a further CH resonance may be masked by the C_5H_5 resonances. ^{19}F NMR spectrum ($CDCl_3$): CF_3 resonances at δ −49.9 (m, 1F), −51.4 (m, 10F), −53.1 (m, 1F). ^{19}F NMR spectrum (acetone-d_6): CF_3 resonances at δ −51.3 (qd with Pt satellites, ^5J(F–F) = 12 Hz, J(Rh–F) = 3 Hz, J(Pt–F) = 65 Hz, 3F), −49.9 (s br, 6F), −48.3 (qd, ^5J(F–F) = 12 Hz and J(Rh–F) = 3 Hz, 3F). ^{13}C NMR spectrum (acetone-d_6): δ 94.1 (s, olefinic CH of COD), 90.6 (d, J(Rh–C) = 3 Hz, C_5H_5), 87.9 (d, J(Rh–C) = 3–4 Hz, C_5H_5), 84.3 (d, J(Rh–C) = 5–6 Hz, C_5H_5), 77.9 (s, olefinic CH of COD), 35.9, 35.5, and 26.5 (3 × s, CH_2 of COD); the CO resonance was not detected; variable temperature ^1H and ^{19}F NMR spectra were recorded and are discussed in the text.

The reaction solution was evaporated to dryness. TLC of a solution of the residue with hexane/diethyl ether (1:1) as eluent separated small amounts of the following compounds: $(C_5H_5)_2Rh_2(CO)_2(CF_3C_2CF_3)$, $(C_5H_5)_2Rh_2Pt(CO)(CF_3C_2CF_3)(COD)$, $(C_5H_5)_3Rh_3(CO)(CF_3C_2CF_3)$ and $(C_5H_5)_4Rh_4Pt(CO)_2(CF_3C_2CF_3)_2$. These were identified from their spectroscopic properties and R_f values.

Reaction of $(\eta$-$C_5H_5)_2Rh_2(CO)(CF_3C_2CF_3)$ (1) with $Pt(COD)_2$, 2:1 ratio

A solution of $Pt(COD)_2$ (0.088 g) in hexane (30 ml) was added slowly to a stirred solution of 1 (0.268 g; mol ratio 1:2) in hexane (30 ml). The reaction flask was kept in the dark. After 3 days, deposition of crystals was complete and two crystal types were evident. The large rhomboids were $(C_5H_5)_2Rh_2Pt(CO)(CF_3C_2CF_3)(COD)$, and the needle aggregates were identified (see below) as $(C_5H_5)_4Rh_4Pt(CO)_2(CF_3C_2CF_3)_2$. The product mixture was conveniently separated by chromatography. Thus, solvent was removed from the reaction mixture, the residue was dissolved in dichloromethane, and the resulting solution was chromatographed by TLC with a 1:1 mixture of diethyl ether and hexane as eluent. This separated two major bands, one green and the other black. After extraction, the individual bands were rechromatographed with a 1:1 mixture of ethyl acetate and hexane as eluent. Extraction of the green band and removal of solvent gave $(C_5H_5)_2Rh_2Pt(CO)(CF_3C_2CF_3)(COD)$ (0.028 g, 7%) which was identified from its melting point and spectroscopic properties.

Extraction of the black band from the TLC plate and evaporation of solvent yielded a dark coloured solid. This was recrystallized from dichloromethane/hexane, and more slowly from a concentrated solution in dichloromethane/diethyl ether/hexane at −30°C for 1 week to give small black crystals of $(C_5H_5)_4Rh_4Pt(CO)_2(CF_3C_2CF_3)_2$ (0.057 g, 18%), m.p. 228°C. Anal. Found: C, 28.7; H, 1.9; F, 18.2. $C_{30}H_{20}F_{12}O_2PtRh_4$ calc.: C, 28.9; H, 1.6; F, 18.3%. Mass spectrum, m/z (relative intensity, assignment): 1191 (4%, M − 2CO), 666 (20%, $[(C_5H_5)_3Rh_3(CF_3C_2CF_3)]^+$), 233 (100%, $C_{10}H_{10}Rh^+$); FAB mass spectrum ($CHCl_3$, NOBA, positive ion): 1247 (2%, M). Infrared spectrum: ν(CO) at 1874vs (KBr) or 1860vs (CH_2Cl_2 soln.) cm^{-1}. ^1H NMR spectrum ($CDCl_3$): C_5H_5 resonances at δ 5.49 (s, 5H) and 5.42 (s, 5H). ^{19}F NMR spectrum ($CDCl_3$): CF_3 resonances at δ −47.3 (m, 3F) and −56.4 (m, 3F).

Preparation of $(C_5H_5)_4Rh_4Pt(CO)_2(CF_3C_2CF_3)_2$ from 1 and $Pt(NBE)_3$

A mixture of **1** (0.104 g, 0.20 mmol) and $Pt(NBE)_3$ (0.095 g, 0.22 mmol) in hexane (20 ml) was stirred for 2 days. The black precipitate was isolated by filtration and identified spectroscopically as $(C_5H_5)_4Rh_4Pt(CO)_2(CF_3C_2CF_3)_2$ (0.105 g, 85%).

Crystallography, $(C_5H_5)_2Rh_2Pt(CO)(CF_3C_2CF_3)(COD)$

A representative crystal was selected directly from the batch deposited in the reaction solution. A dark red tabular crystal was used for data collection. Intensity measurements were made on a Nicolet R3m/V diffractometer with graphite monochromated Mo-K_α radiation at 22°C. Cell parameters were derived by least-squares calculations from angular settings of 30 reflections measured between $5° < 2\theta < 26°$. Other crystal data are summarized in Table 1. Three standard reflections monitored every 197 reflections showed no significant variation in intensity over the data collection period.

Intensity data were corrected for Lorentz and polarization effects. A numerical absorption correction was applied [8], the maximum and minimum transmission

Table 1

Summary of crystal structure data for the complexes $(C_5H_5)_2Rh_2Pt(CO)(CF_3C_2CF_3)(COD)$ and $(C_5H_5)_4Rh_4Pt(CO)_2(CF_3C_2CF_3)_2$

(a) *Crystal data*		
Formula	$C_{23}H_{22}F_6OPtRh_2$	$C_{30}H_{20}F_{12}O_2PtRh_4$
Mol wt	829.3	1247.2
Crystal size (mm)	0.36×0.36×0.16	0.14×0.11×0.04
Crystal system	Monoclinic	Monoclinic
Space group	$C2/c$	$P2_1$
a (Å)	27.654(5)	11.796(6)
b (Å)	8.733(2)	15.178(7)
c (Å)	18.622(5)	9.765(5)
β (deg)	93.86	113.32
V (Å^3)	4487(2)	1605(2)
Z	8	2
D (calc.) (g cm^{-3})	2.46	2.58
D (meas.) (g cm^{-3})	2.45(2)	2.57(2)
F(000)	3120	1164
Mo-K_α radiation, λ (Å)	0.71073	0.7107
μ(Mo-K_α) (cm^{-1})	77.8	64.7
(b) *Data collection*		
Temperature (°C)	20(1)	20(1)
2θ limits (deg)	5–26	6–60
ω-scan angle (deg)	$\pm(1.20+0.3\tan\theta)$	$\pm(1.30+0.2\tan\theta)$
Scan rate (deg min^{-1})	3.00–19.53	2.70
Total no. of data	6546	4836
No. of data, $F > 6\sigma F$	5061	
No. of data, $I > 3\sigma I$		3328
Abs cor	0.888 (max), 0.815 (min)	0.771 (max), 0.488 (min)
Final R and R_w	0.041 and 0.061	0.057 and 0.061
Weight w	$[\sigma^2(F_o)+0.0035F^2]^{-1}$	$[\sigma^2(F_o)]^{-1}$

Table 2

Final positional parameters for $(\eta\text{-}C_5H_5)_2Rh_2Pt(CO)(CF_3C_2CF_3)(COD)$ (2) and $(\eta\text{-}C_5H_5)_4Rh_4Pt(CO)_2(CF_3C_2CF_3)_2$ (3)

Atom	x	y	z
(a) *Atomic coordinates (× 10⁴) for* $(\eta\text{-}C_5H_5)_2Rh_2Pt(CO)(CF_3C_2CF_3)(COD)$ *(2)*			
Pt(1)	979(1)	1651(1)	156(1)
Rh(1)	1184(1)	2102(1)	1539(1)
Rh(2)	2030(1)	1134(1)	1141(1)
O(1)	1763(2)	4318(7)	731(3)
F(1)	1611(3)	−2596(6)	1604(3)
F(2)	894(2)	−1833(8)	1773(4)
F(3)	1490(2)	−1028(7)	2438(3)
F(4)	1695(2)	−1011(7)	−596(3)
F(5)	1962(2)	−2216(6)	353(3)
F(6)	1212(2)	−2380(6)	−34(4)
C(1)	1353(3)	−1346(9)	1755(4)
C(2)	1398(2)	−29(8)	1253(4)
C(3)	1442(2)	−36(8)	505(3)
C(4)	1576(3)	−1391(9)	72(4)
C(5)	1674(3)	3109(8)	939(4)
C(6)	307(3)	3067(9)	−7(4)
C(7)	694(3)	4029(9)	−99(4)
C(8)	883(3)	4490(11)	−811(5)
C(9)	908(3)	3156(9)	−1362(5)
C(10)	1012(3)	1616(8)	−1041(4)
C(11)	664(3)	604(9)	−864(4)
C(12)	131(3)	903(10)	−910(5)
C(13)	−33(3)	2444(12)	−637(5)
C(14)	1129(3)	3955(12)	2361(5)
C(15)	725(3)	4036(11)	1911(5)
C(16)	476(4)	2632(12)	1969(5)
C(17)	731(4)	1704(11)	2497(5)
C(18)	1139(4)	2518(12)	2741(5)
C(19)	2660(4)	758(12)	1991(6)
C(20)	2655(4)	−391(13)	1512(6)
C(21)	2732(3)	204(11)	822(5)
C(22)	2780(4)	1785(11)	899(6)
C(23)	2706(3)	2158(12)	1622(5)
(b) *Atomic parameters for* $(\eta\text{-}C_5H_5)_4Rh_4Pt(CO)_2(CF_3C_2CF_3)_2$ *(3)*			
Pt	0.25347(5)	0.5	0.30757(6)
Rh(1)	0.4135(1)	0.4081(1)	0.2269(2)
Rh(2)	0.0906(1)	0.4680(1)	0.4256(1)
Rh(3)	0.0222(1)	0.4474(1)	0.1292(1)
Rh(4)	0.4370(1)	0.5833(1)	0.2703(2)
C(1)	0.1587(15)	0.6727(12)	0.4085(20)
C(2)	0.1284(13)	0.5831(10)	0.3401(16)
C(3)	0.0095(12)	0.5524(9)	0.2550(15)
C(4)	−0.1093(16)	0.6013(12)	0.2182(21)
C(5)	0.4635(17)	0.5568(13)	0.6166(22)
C(6)	0.4333(14)	0.5251(10)	0.4577(18)
C(7)	0.5080(13)	0.4805(9)	0.4104(17)
C(8)	0.6482(19)	0.4674(15)	0.5009(25)
C(9)	0.1087(15)	0.5222(11)	0.0548(20)
C(10)	0.3230(15)	0.3582(11)	0.3349(19)
C(11)	0.1955(16)	0.3941(13)	0.6343(22)

Table 2 (continued)

Atom	x	y	z
(b) *Atomic parameters for* $(\eta\text{-}C_5H_5)_4Rh_4Pt(CO)_2(CF_3C_2CF_3)_2$ *(3)*			
C(12)	0.0974(16)	0.3449(12)	0.5411(21)
C(13)	−0.0152(17)	0.3847(13)	0.5204(22)
C(14)	0.0092(19)	0.4670(15)	0.5934(24)
C(15)	0.1470(17)	0.4749(13)	0.6660(23)
C(16)	−0.1599(22)	0.4005(17)	−0.0233(29)
C(17)	−0.0767(25)	0.3756(19)	−0.0843(33)
C(18)	0.0136(20)	0.3111(15)	0.0298(26)
C(19)	−0.0294(21)	0.3046(16)	0.1335(27)
C(20)	−0.1336(23)	0.3614(17)	0.1033(30)
C(21)	0.5396(18)	0.3923(15)	0.1102(25)
C(22)	0.4218(21)	0.4116(17)	−0.0010(28)
C(23)	0.3398(19)	0.3471(14)	−0.0022(24)
C(24)	0.4024(19)	0.2827(15)	0.1047(25)
C(25)	0.5281(21)	0.3097(15)	0.1699(27)
C(26)	0.5267(20)	0.6439(15)	0.1304(25)
C(27)	0.3919(19)	0.6606(14)	0.0617(24)
C(28)	0.3590(18)	0.7120(13)	0.1538(23)
C(29)	0.4662(22)	0.7259(15)	0.2929(28)
C(30)	0.5715(20)	0.6845(15)	0.2718(26)
O(1)	0.1279(13)	0.5635(10)	−0.0351(16)
O(2)	0.2925(13)	0.2989(10)	0.3852(17)
F(1)	0.1355(10)	0.6816(8)	0.5333(13)
F(2)	0.2772(11)	0.6981(8)	0.4463(14)
F(3)	0.0895(11)	0.7358(8)	0.3135(15)
F(4)	−0.1393(13)	0.6520(9)	0.0978(16)
F(5)	−0.2053(11)	0.5455(8)	0.1817(14)
F(6)	−0.1120(12)	0.6496(9)	0.3294(15)
F(7)	0.5321(11)	0.5015(11)	0.7163(15)
F(8)	0.3683(11)	0.5782(8)	0.6496(13)
F(9)	0.5308(12)	0.6337(9)	0.6443(15)
F(10)	0.6665(10)	0.3930(8)	0.5858(14)
F(11)	0.7037(12)	0.5298(9)	0.5921(16)
F(12)	0.7077(12)	0.4517(9)	0.4097(16)

factors being 0.888 and 0.815, respectively. The atomic scattering factors for neutral atoms were taken from reference [9] and were corrected for anomalous dispersion by using values from the same reference. All calculations were performed on a MicroVAX 2000 computer. The program used for least-squares refinement was that due to Sheldrick [8].

The structure was solved by direct methods and refinement effected by full-matrix least-squares methods. Anisotropic thermal parameters were introduced for Pt, Rh, and F. Isotropic thermal parameters were assigned to all other atoms. Hydrogen atoms were located in geometrically idealized positions (C–H = 0.96 Å) with a single fixed isotropic thermal parameter.

Crystallography, $(C_5H_5)_4Rh_4Pt(CO)_2(CF_3C_2CF_3)_2$

A representative red-black tabular crystal was chosen and used for data collection. Intensity measurements were made on a Philips PW 1100 diffractometer using graphite monochromated Mo-K_α radiation with $6° < 2\theta < 60°$. Cell parame-

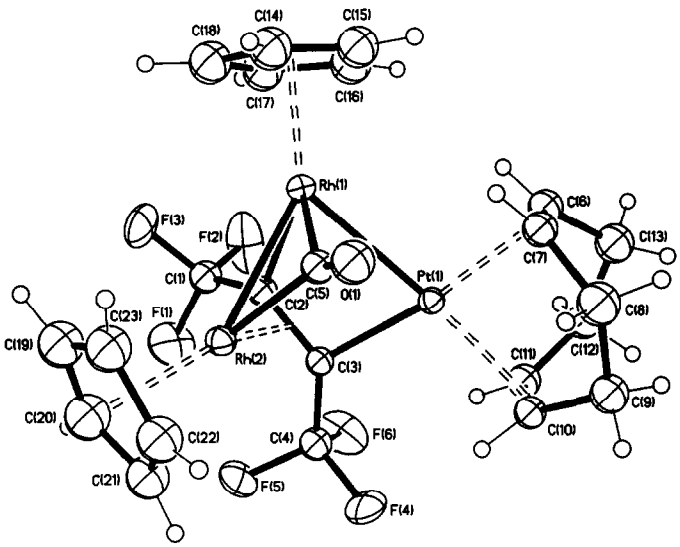

Fig. 1. Molecular structure of the complex $(\eta\text{-}C_5H_5)_2Rh_2Pt(CO)(CF_3C_2CF_3)(COD)$ (2).

ters were determined from 24 accurately centred reflections and were calculated by the standard Philips program. Other crystal data are summarized in Table 1. Inversion of the atom coordinates to check the absolute configuration gave $R = 0.045$, $wR = 0.045$. Three standard reflections monitored every 5 h showed no significant variation in intensity over the data collection period.

Intensity data were processed as described previously [10]. A numerical absorption correction was applied, the maximum and minimum transmission factors being 0.771 and 0.488, respectively. The atomic scattering factors for neutral atoms were taken from ref. 9 and were corrected for anomalous dispersion using values taken from the same reference. All calculations were performed on a VAX 11/780 computer. The program used for least-squares refinement was that due to Sheldrick [11].

The structure was solved by conventional Patterson and Fourier techniques. Full-matrix least-squares refinement was achieved with anisotropic thermal parameters for Pt and Rh and isotropic thermal parameters for all other non-hydrogen atoms.

Final positional parameters for both complexes are given in Table 2. Figures 1 and 2 show the atomic labelling schemes used, and selected bond lengths and angles are listed in Table 3. Listings of structure factor amplitudes, thermal parameters, and ligand geometries for each complex are available from the authors.

Results

Formation and spectroscopic properties of the Rh_2Pt cluster

When a 1:1 mixture of **1** and $Pt(COD)_2$ in hexane was stirred at room temperature with exclusion of light, a green-black crystalline product formed slowly. It was formulated as $(C_5H_5)_2Rh_2Pt(CO)(CF_3C_2CF_3)(COD)$ (**2**) from

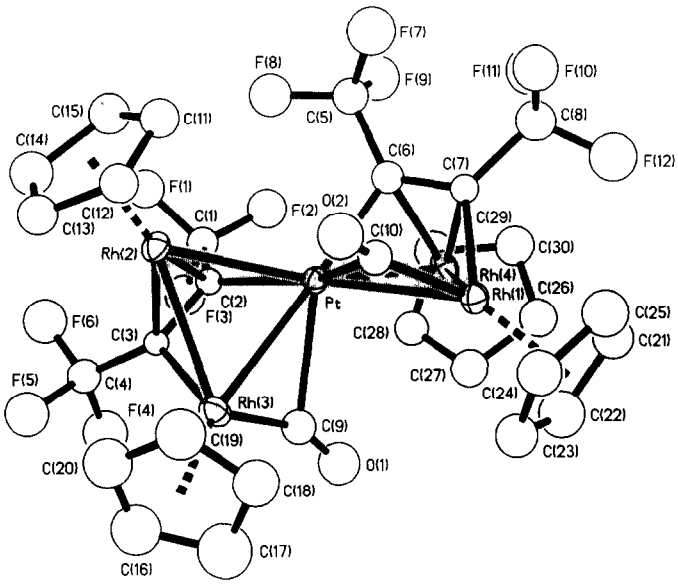

Fig. 2. Molecular structure of the complex $(\eta\text{-}C_5H_5)_4Rh_4Pt(CO)_2(CF_3C_2CF_3)_2$ (**3**).

microanalysis and mass spectral data. Formation of the heteronuclear cluster has involved replacement of one *COD* ligand on $Pt(COD)_2$ by the complete dinuclear complex $(C_5H_5)_2Rh_2(CO)(CF_3C_2CF_3)$. The reaction was done in the dark to inhibit a competing and more rapid reaction which is known [12] to occur when a solution containing **1** and cyclooctadiene is exposed to sunlight; this reaction gives $(C_5H_5)_2Rh_2(CF_3C_2CF_3 \cdot H)(COD\text{-}H)$.

Solid samples of **2** are stable in air. The compound is soluble in common organic solvents except saturated hydrocarbons, but the green solutions liberate cyclooctadiene very slowly. The infrared spectrum of **2** showed a strong absorption at 1789 (KBr) or 1761 cm^{-1} (CH_2Cl_2 solution) which is assigned to a face-bridging carbonyl. The ^1H and ^{19}F NMR spectra are solvent dependent, with greater complexity evident in acetone compared to chloroform. These spectra are discussed in some detail below, but in general terms they indicate the co-existence of two isomers with the proportions being dependent on both solvent and temperature. As an aid to interpreting the spectroscopic data, it was decided to determine the crystal and molecular structure of the complex; this is discussed below.

Formation and spectroscopic properties of the Rh_4Pt cluster

A similar reaction between **1** and $Pt(COD)_2$, but with a 2:1 mol ratio of reactants, gave **2** and another major product **3**. They were separated by chromatography, and small black crystals of **3** were obtained by recrystallization. Microanalysis, supported by a FAB mass spectrum, indicated the formula $(C_5H_5)_4Rh_4Pt(CO)_2(CF_3C_2CF_3)_2$ for **3**. Thus, in the formation of this complex, both COD ligands have been displaced from the $Pt(COD)_2$. The complex **3** was also obtained when a solution of **1** and the norbornene complex $Pt(NBE)_3$ was stirred at room temperature. Indeed, this proved to be the best route to **3**, with an 85% yield being obtained after 2 days. The compound is insoluble in saturated

Table 3

Some important bond lengths (Å) and angles (deg) for $(\eta\text{-}C_5H_5)_2Rh_2Pt(CO)(CF_3C_2CF_3)(COD)$ (2) and $(\eta\text{-}C_5H_5)_4Rh_4Pt(CO)_2(CF_3C_2CF_3)_2$ (3)

(a) *Bond lengths*

Complex 2		Complex 3			
Rh(1)–Rh(2)	2.641(1)	Rh(1)–Rh(4)	2.690(2)	Rh(2)–Rh(3)	2.697(2)
Pt(1)–Rh(1)	2.628(1)	Pt–Rh(4)	2.654(2)	Pt–Rh(2)	2.647(1)
Pt(1) ··· Rh(2)	3.361(4)	Pt–Rh(1)	2.703(1)	Pt–Rh(3)	2.712(1)
Rh(1)–C(2)	2.035(7)	Rh(1)–C(7)	2.02(1)	Rh(3)–C(3)	2.05(1)
Rh(2)–C(2)	2.044(7)	Rh(4)–C(7)	2.03(1)	Rh(2)–C(3)	2.02(1)
Rh(2)–C(3)	2.198(6)	Rh(4)–C(6)	2.05(2)	Rh(2)–C(2)	2.06(2)
Pt–C(3)	2.029(6)	Pt–C(6)	2.08(1)	Pt–C(2)	2.06(2)
C(2)–C(3)	1.406(9)	C(6)–C(7)	1.33(2)	C(2)–C(3)	1.40(2)
Rh(1)–C(5)	2.014(7)	Rh(1)–C(10)	1.93(2)	Rh(3)–C(9)	1.86(2)
Rh(2)–C(5)	2.009(7)	Rh(4) ··· C(10)	3.81(2)	Rh(2) ··· C(9)	3.80(2)
Pt(1)–C(5)	2.658(8)	Pt–C(10)	2.28(2)	Pt–C(9)	2.40(2)
O(1)–C(5)	1.157(10)	O(2)–C(10)	1.15(2)	O(1)–C(9)	1.17(2)
Pt(1)–C(6)	2.236(8)				
Pt(1)–C(7)	2.261(8)				
Pt(1)–C(10)	2.236(7)				
Pt(1)–C(11)	2.231(7)				

(b) *Bond angles*

Complex 2		Complex 3			
Pt(1)–Rh(1)–Rh(2)	79.3(1)	Pt–Rh(1)–Rh(4)	58.9(0)	Pt–Rh(2)–Rh(3)	61.0(0)
		Pt–Rh(4)–Rh(1)	60.8(0)	Pt–Rh(3)–Rh(2)	58.6(0)
		Rh(1)–Pt–Rh(4)	60.3(0)	Rh(2)–Pt–Rh(3)	60.4(0)
Pt(1)–Rh(1)–C(2)	69.8(2)	Pt–Rh(1)–C(7)	70.4(5)	Pt–Rh(3)–C(3)	71.3(4)
Rh(2)–Rh(1)–C(5)	48.9(2)	Pt–Rh(1)–C(10)	56.1(5)	Pt–Rh(3)–C(9)	60.1(5)
Rh(1)–Rh(2)–C(5)	49.1(2)	Rh(1)–Pt–C(10)	44.5(5)	Rh(3)–Pt–C(9)	42.0(5)
Rh(1)–Pt(1)–C(3)	72.9(2)	Rh(1)–Pt–C(6)	70.4(5)	Rh(3)–Pt–C(2)	71.3(4)
Rh(1)–C(2)–C(1)	120.2(5)	Rh(1)–C(7)–C(8)	121.7(12)	Pt–C(2)–C(1)	124.6(11)
Rh(1)–C(2)–C(3)	108.0(5)	Rh(1)–C(7)–C(6)	112.1(11)	Pt–C(2)–C(3)	108.4(11)
C(1)–C(2)–C(3)	129.3(6)	C(6)–C(7)–C(8)	124.9(15)	C(1)–C(2)–C(3)	125.1(14)
Pt(1)–C(3)–C(2)	102.7(4)	Pt–C(6)–C(5)	122.4(11)	Rh(3)–C(3)–C(2)	108.7(11)
Pt(1)–C(3)–C(4)	125.2(5)	Pt–C(6)–C(7)	107.0(10)	Rh(3)–C(3)–C(4)	121.6(9)
C(2)–C(3)–C(4)	125.4(6)	C(7)–C(6)–C(5)	126.4(15)	C(2)–C(3)–C(4)	126.9(13)
Rh(1)–C(5)–Rh(2)	82.0(3)	Rh(1)–C(10)–Pt	79.4(6)	Rh(3)–C(9)–Pt	77.9(6)
Rh(1)–C(5)–O(1)	138.7(6)	Rh(1)–C(10)–O(2)	151.2(17)	Rh(3)–C(9)–O(1)	156.9(13)
Rh(2)–C(5)–O(1)	137.1(6)	Pt–C(10)–O(2)	129.1(16)	Pt–C(9)–O(1)	125.1(12)

hydrocarbons, but dissolves readily in polar organic solvents. There is slow decomposition when the solutions are exposed to the air, but the solid samples are air stable.

The infrared spectrum of a solution of **3** in dichloromethane showed an edge-bridging carbonyl absorption at 1862 cm^{-1}. Two closely spaced C_5H_5 resonances of equal intensity, and two CF_3 resonances also of equal intensity, were observed in the ^1H and ^{19}F NMR spectra, respectively; these spectra were not solvent or temperature dependent. In the lower field CF_3 resonance, Pt–F coupling of 67 Hz was evident, and this is typical of ^4J coupling. The cumulative data indicate an unsymmetrical attachment of the hexafluorobut-2-yne ligand within the

molecule, but to determine the precise ligand arrangement a crystal structure determination was undertaken.

Crystal and molecular structures of $(\eta\text{-}C_5H_5)_2Rh_2Pt(CO)(CF_3C_2CF_3)(COD)$ *(2) and* $(\eta\text{-}C_5H_5)_4Rh_4Pt(CO)_2(CF_3C_2CF_3)_2$ *(3)*

A preliminary account of the formation and structure of the pentanuclear cluster **3** has been published [13]. This compound has two Rh_2Pt triangles linked through a common platinum atom. There is a dihedral angle of 70.0° between the trinuclear planes. All the Rh–Rh and Rh–Pt distances are consistent with single bond interactions, but a difference of about 0.05 Å is found for the two Rh–Pt distances in each triangle. A carbonyl spans each of the longer Rh–Pt bonds, but the angles around the carbonyl carbon indicate that the attachment is asymmetric. Indeed, the Rh–C–O angle is only 23° from the linear arrangement expected for a terminal attachment of the carbonyl to rhodium. The asymmetry is also reflected in the metal–carbonyl bond lengths, with the Rh–C(O) distances being about 0.45 Å shorter than the Pt–C(O) distances. The observed Rh–C(O) distances are intermediate between those found for Rh–CO(terminal) in $(\eta\text{-}C_5H_5)_2Rh_2(CO)_2(CF_3C_2CF_3)$ (1.82(1) Å) [14] and for Rh–CO(bridging) in $(\eta\text{-}C_5H_5)_2Rh_2(\mu\text{-}CO)(CF_3C_2CF_3)$ (2.005(5) Å) [15]. The Pt–C(O) distance of 2.35 Å (mean) is significantly longer than the distance normally found for Pt–μ_2-CO (*e.g.* 2.03 Å in $NiPtCl_2(\mu\text{-}CO)(\mu\text{-dppm})_2$) [16]. There have been some previous reports of semi-bridging attachments of this type, and it is thought [17] that they compensate for what would be a highly polarized M–M′ bond if the carbonyls were terminal. The very long distance from the carbonyl carbon to the other rhodium atom (mean, 3.81(2) Å) precludes description of the attachment as semi-facebridging. The hexafluorobut-2-yne is face bridging and is σ-bonded to that Rh–Pt edge which has the bridging carbonyl and π-bonded to the remaining rhodium atom. The alkyne C–C bond is essentially parallel to the Rh–Pt bond. This μ_3-(η^2-//) mode of attachment is similar to that observed in numerous alkyne-M_3 clusters [18]. There are no unusual bond parameters associated with the alkyne attachment. Within each half of the molecule, the alkyne and the carbonyl are on the same side of the Rh_2Pt plane. Each of the cyclopentadienyl rings is η^5-attached to a rhodium and again there are no exceptional features in the bond parameters.

The non-closure of the Rh_2Pt triangle is a major difference in the structure of the trinuclear cluster **2** compared to the individual halves of **3**. The non-bonding Rh(2) · · · Pt(1) distance is 3.361(4) Å, and the Pt(1)–Rh(1)–Rh(2) angle has opened out from about 60° in **3** to about 80° in **2**. The Rh(1)–Rh(2) and Pt(1)–Rh(1) distances in **2** are slightly shorter than the comparable distances in **3** but fall within the ranges normally associated with metal–metal single bonds for these metals. The carbonyl is symmetrically attached to the Rh(1)–Rh(2) bond, with a mean Rh–C(O) distance of 2.01(1) Å and a mean Rh–C–O angle of 137.9(6)°. This bridging carbonyl leans towards the platinum, and the Pt(1) · · · C(5) distance is 2.658(8) Å. Although this is 0.55 Å longer than the Rh–C(O) distances, it does seem reasonable to regard the carbonyl as semi-face bridging. This is supported by the infrared spectrum (ν(CO) is at 1789 cm^{-1} for a solid sample in a KBr disk) and by comparisons with related clusters. In some other clusters with Rh_2Pt faces and semi-triply bridging carbonyls, the longest M–C(O) bonds are to Pt and fall within the range 2.52–2.56(2) Å [19]. In another heteronuclear cluster,

$(\eta\text{-}C_5H_5)_2Mo_2Pt_2(\mu\text{-}CO)_6(PEt_3)_2$, the platinum to semi-face bridging carbonyl distances average 2.69 Å [20]. The hexafluorobut-2-yne ligand in **3** is again attached in the $\mu_3\text{-}(\eta^2\text{-}//)$ mode. It is σ-bonded to Pt(1) and Rh(1) with the C(2)–C(3) bond essentially parallel to the Pt(1)–Rh(1) bond, and π-bonded to Rh(2). The latter attachment is somewhat asymmetric, with the distance to C(3) being 0.15 Å greater than that to C(2). This can be attributed to the geometric consequences of the open Rh_2Pt core structure. Each cyclopentadienyl group is η^5-attached to a rhodium atom, and there is an η^4-attachment of the cyclooctatetraene ligand to platinum. None of the M–C or C–C distances is unusual.

Spectroscopic properties and solution structures of the complexes

The spectroscopic properties indicate that the solid state structure of **3** is retained in solution. However, the spectra of solutions of **2** show both solvent and temperature dependence and are indicative of the co-existence of two isomers.

The ^1H NMR spectrum of a solution of **2** in $CDCl_3$ is difficult to interpret due to the overlap of signals for the cyclopentadienyl and cyclooctatetraene protons. In acetone-d_6, three cyclopentadienyl resonances of relative intensity 1:1:2 are clearly discernable, and the cyclooctatetraene regions of the spectrum are relatively complex. Information about the number of species in solution is more easily extracted from the ^{19}F NMR spectra. For solutions in $CDCl_3$, three trifluoromethyl resonances are observed in an approximate ratio of 1:20:1. The most intense peak at δ −51.4 is broad and featureless, and the remaining pair of peaks at δ −49.5 and −53.1 are complex multiplets. A similar spectrum was observed for solutions in acetone-d_6 except that the relative intensity of the signals is 1:2:1. The resonances at δ −48.3 and −51.3 are quartets of doublets with F–F and Rh–F coupling constants of 12 and 3 Hz, respectively. The presence of platinum satellites with J(Pt–F) = 65 Hz adds extra complexity to the peak at higher field. The central peak is again broad and featureless. These data indicate that two isomers (A and B) coexist in solution, with the proportions of A and B being 1:10 in chloroform and 1:1 in acetone. We suggest that A has a structure analogous to the observed solid state structure, and that B has a related but fluxional structure in solution. A reasonable structure to propose for B is that shown in Fig. 3 in which there is a closed Rh_2Pt core.

Low temperature ^{19}F NMR spectra were recorded for **2** in acetone-d_6. As the temperature is decreased, the central peak becomes broader and at 253 K it separates into two peaks of equal intensity at δ −48.9 and −49.3. In the spectrum at 223 K, these signals are readily identified as quartets with F–F coupling of 11 Hz, and there are ^{195}Pt satellites (J(Pt–F) = 83 Hz) on the lower field signal. The resonances associated with isomer A at δ −51.3 and −48.3 remain relatively unchanged as the temperature is lowered except that the doublet pattern previously evident in the lower field peak is no longer detected. Similar effects were observed in the variable temperature ^1H NMR spectra of **2** in acetone-d_6. One of the three cyclopentadienyl resonances (δ 5.60) seen at room temperature broadens on cooling and at 238 K separates into two peaks of equal intensity; this is assigned to isomer B. The other two peaks (δ 5.44 and 5.33) did not change as the temperature was lowered and these are associated with isomer A. It is evident from these data that the structure of isomer A is static in solution over the temperature range studied, but for B there is rotation of the alkyne on the Rh_2Pt

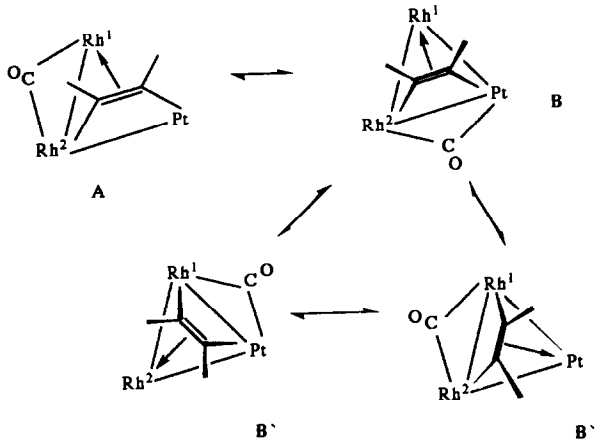

Fig. 3. A scheme for the interconversions between isomers of **2**. The carbonyls are probably semi-face bridging, but for clarity they are shown as edge bridging. The groups C_5H_5, COD and CF_3 are also omitted for clarity.

face. To account for the averaging of the CF_3 signals in the spectra of B, complete rotation rather than a "windshield-wiper" motion of the alkyne must be invoked.

Discussion

The displacement of weakly coordinating ligands is now a relatively common approach to cluster synthesis. It offers the advantages of mild reaction conditions and ease of control of the stoichiometry of the cluster forming reaction. Stone pioneered this approach a decade ago, using $Pt(COD)_2$ and related compounds as the source of Pt^0 to prepare several heteronuclear clusters containing platinum [19,21]. Others have followed similar procedures, and a very recent example involves the formation of $Pt_3Fe_3(CO)_{15}$ and related Pt–Fe clusters from $Pt(COD)_2$ and $Fe(CO)_5$ [22].

The reactions described in this paper were achieved at room temperature and allowed the addition of one or two units of the Rh_2 compound to Pt depending on the ratio of the reactants. The best yields of the Rh_2Pt and Rh_4Pt products obtained were 42 and 18%, respectively. However, by using $Pt(NBE)_3$ in place of $Pt(COD)_2$, the yield of **3** was substantially increased to 85%; this is consistent with the very weak alkene–platinum bonding in the norbornene complex. In some related studies, we have found that **3** is also formed in reactions between **1** and platinum(II) compounds such as (hexadiene)$PtCl_2$. Other products that are formed in these interesting redox reactions have not yet been fully characterized.

In our systems, the formation of new Rh–Pt bonds is accompanied by a reorientation of the alkyne that was initially attached to the Rh–Rh bond. In both cluster products, the face bridging alkyne prefers to be σ-attached to Pt and one Rh and π-bonded to the remaining Rh. This is consistent with a reaction pathway involving nucleophilic attack of the d^{10} platinum centre on a σ^*-orbital of the rhodium–alkyne interaction; the latter is calculated [23] to be the LUMO for **1**.

A special feature of the structure of **2** is the ease with which interconversion between closed and open forms of the cluster core occurs when the complex is in

solution. The interconversion involves the facile making and breaking of a Rh–Pt bond, and it is interesting to reflect on possible reasons for this phenomenon. According to the Wade–Mingos rules [24], a trinuclear cluster with three M–M bonds will generally have a 48-electron count. However, many Pt_3 clusters have their full complement of Pt–Pt bonds even when the cluster electron count is only 42; this is a consequence of the tendency for an individual platinum(0) to adopt a 16 rather than an 18 electron configuration [25]. On this basis, we could regard the normal electron count for a Rh_2Pt cluster to be either 48 or 46 electrons. Since M–M bond making and breaking in cluster chemistry is often accomplished by deliberately adding electron pairs to or subtracting them from the cluster core, the observed behaviour of **2** may be attributed to this ambivalence of platinum. In B it is acting as a conventional 18 electron centre, but in A it is behaving as a 16 electron centre with the two additional electrons then causing the loss of a metal–metal bond.

Acknowledgements

This work was supported by grants from the Australian Research Grants Scheme. We are grateful to Johnson Matthey Technology Centre for the loan of rhodium trichloride.

References

1 R.D. Adams, in D.F. Shriver, H.D. Kaesz and R.D. Adams (Eds.), The Chemistry of Metal Cluster Complexes, VCH Publishers, New York, 1990, Chapter 3, pp. 121–170.
2 A.S. Katugin, A.A. Pasynskii, I.L. Eremenko, B. Orazsakhatov, A.S. Aliev, Yu T. Struchkov and A.I. Yanovsky, J. Organomet. Chem., 382 (1990) 423; see also refs. 1–6 cited in this paper.
3 R.S. Dickson, O.M. Paravagna and H. Pateras, Organometallics, 9 (1990) 2780.
4 W.L. Amarego, D.D. Perrin and D.R. Perrin, Purification of Laboratory Chemicals, 2nd edition, Pergamon, Oxford, UK, 1980.
5 R.S. Dickson, S.H. Johnson and G.N. Pain, Organomet. Synth., 4 (1988) 283.
6 I.A. Zakharova, J. Organomet. Chem., 72 (1974) 283.
7 M. Green, J.A.K. Howard, J.L. Spencer and F.G.A. Stone, J. Chem. Soc., Dalton Trans., (1977) 271.
8 G.M. Sheldrick, SHELXTL PLUS, Revision 3.4, Siemens Analytical X-Ray Instruments Inc., Madison, WI, 1988.
9 J.A. Ibers and W.C. Hamilton (Eds.), International Tables for X-Ray Crystallography, Vol. IV, Kynoch Press, Birmingham, UK, 1974.
10 G.D. Fallon and B.M. Gatehouse, J. Solid State Chem., 34 (1980) 193.
11 G.M. Sheldrick, SHELX-76, Program for Crystal Structure Determination, Cambridge UK, 1975.
12 R.S. Dickson, S.M. Jenkins, B.W. Skelton and A.H. White, Polyhedron, 7 (1988) 859.
13 R.S. Dickson, G.D. Fallon, M.J. Liddell, B.W. Skelton and A.H. White, J. Organomet. Chem., 327 (1987) C51.
14 R.S. Dickson, S.H. Johnson, H.P. Kirsch and D.J. Lloyd, Acta Crystallogr., B33 (1977) 2057.
15 R.S. Dickson, G.N. Pain and M.F. Mackay, Acta Crystallogr., B35 (1979) 2321.
16 D.G. Holah, A.N. Hughes, V.R. Magnuson, H.A. Mirza and K.O. Parker, Organometallics, 7 (1988) 1233.
17 C.M. Lukehart, Fundamental Transition Metal Organometallic Chemistry, Brooks/Cole, California, 1985, pp. 41–44.
18 See, for example; R.S. Dickson and O.M. Paravagna, Organometallics, 10 (1991) 721; D. Boccardo, M. Botta, R. Gobetta, D. Osella, A. Tiripicchio and M.T. Camellini, J. Chem. Soc., Dalton Trans., (1988) 1249.
19 M. Green, R.M. Mills, G.N. Pain, F.G.A. Stone and P. Woodward, J. Chem. Soc., Dalton Trans., (1982) 1309; M. Green, J.A.K. Howard, G.N. Pain and F.G.A. Stone, J. Chem. Soc., Dalton Trans., (1982) 1327.

20 A. Bender, P. Braunstein, Y. Dusansoy and J. Protas, J. Organomet. Chem., 172 (1979) C51.
21 F.G.A. Stone, Acc. Chem. Res., 14 (1981) 318; F.G.A. Stone, Inorg. Chim. Acta, 50 (1981) 33.
22 R.D. Adams, I. Arafa, G. Chen, J.-C. Lii and J.-G. Wang, Organometallics, 9 (1990) 2350.
23 D.M. Hoffman, R. Hoffmann and C.R. Fisel, J. Am. Chem. Soc., 104 (1982) 3858.
24 D.M.P. Mingos and A.S. May, in D.F. Shriver, H.D. Kaesz and R.D. Adams (Eds.), The Chemistry of Metal Cluster Complexes, VCH Publishers, New York, 1990, Chap. 2, pp. 11–120.
25 L. Manojlovic-Muir, K.W. Muir, M. Rashidi, G. Schoettel and R.J. Puddephatt, Organometallics, 10 (1991) 1719 and refs. cited therein.